THE UNIVERSITY OF UTAH

THE UNIVERSITY OF UTAH
GLOBAL CHANGE & SUSTAINABILITY CENTER

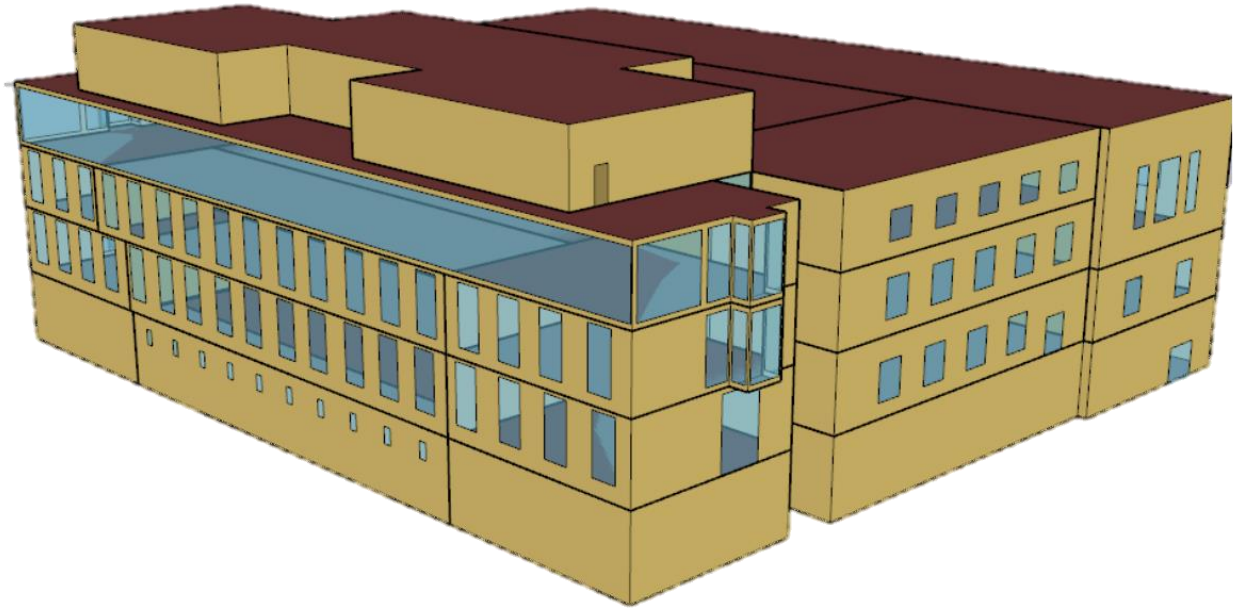

High-Fidelity Building Modeling Enabled Digital Twin Development for Continuous Building and HVAC Monitoring

Prepared For:

SEED2SOIL

Final Report

Aug 2023

ACKNOWLEDGMENTS

We gratefully acknowledge the funding provided by the University of Utah's SEED2SOIL program, with invaluable support from the Global Change and Sustainability Center (GCSC). Their unwavering commitment to advancing our research has been instrumental in the success of this project.

CONTENTS

EXECUTIVE SUMMARY

This report is prepared for the SEED2SOIL project, summarizing the multifaceted activities conducted by our project team. The project encompasses a novel building modeling and calibration framework, building energy auditing, building fault modeling, monitoring platform development, and students engagement.

Novel Bayesian Calibration Framework

Our primary focus is the introduction of a novel Bayesian calibration framework, tailored for high-temporal-resolution calibration of building energy models (BEMs). This framework not only advances the precision of BEM calibration but also integrates fault detection and diagnosis (FDD) strategies to monitor building operation inefficiencies.

Building Audits and Assessments

In collaboration with the University of Utah's Intermountain Industrial Assessment Center (IIAC), we conducted a comprehensive energy audit for the Crocker Science Center (CSC) building. This audit covered facility assessment, operational conditions, energy accounting, waste management, and energy-saving recommendations. The analysis yielded an estimated annual utility savings of $16,162, equivalent to 8.9% of the annual utility bill.

Case Study and Validation

To showcase the effectiveness of our framework, we conducted a comprehensive case study. This involved simultaneous calibration of various parameters within a high-fidelity physics-based model. The model's outputs for heating, cooling, and electricity consumption were validated using real-world data. Our calibration results meet the rigorous hourly calibration requirements defined by ASHRAE Guideline 14.

Fault Detection and Software Development

Our fault monitoring results demonstrate the framework's success in detecting common building operation faults. Furthermore, we have developed specialized software to monitor 7 types

building operation inefficiencies through FDD strategies, further enhancing energy efficiency and fault detection accuracy.

Engagement of Students

One undergraduate student and three PhD students from Department of Civil Engineering and Department of Chemical Engineering have played an instrumental role in our project's success. Their active participation across various project phases, from seminars to energy audits, software development, and paper publications, has enriched their research experience and significantly contributed to our overall achievements.

1.0 INTRODUCTION

1.1 Problem Statement

Building energy consumption accounts for a significant portion, ranging from 20% to 40% of society's overall energy use [1]. With the growing human behavior and increasing demand for building services and comfort, the energy consumption of buildings is expected to continue rising in the future.

Calibrating building energy model is significant to close the discrepancy between modeling and field measurements, thus fundamental to support diverse applications such as monitoring building energy efficiency and fault detection and diagnosis (FDD). Bayesian calibration has emerged as one of the most widely used approaches for effective building calibration. However, current calibration is mostly performed at a low resolution (e.g., annual, or monthly), instead of high resolution, i.e., hourly, which is important for FDD scenarios to capture faults.

Current FDD tools mainly based on machine-learning algorithms hold promise for lowering cost barriers for building operations. However, accessing high-quality fault datasets, which are often difficult to obtain, is necessary for these algorithms.

1.2 Objectives

To address these gaps in research, we present a deep learning-based and computationally efficient Bayesian calibration framework specifically designed for the automated calibration of BEMs at high temporal resolution (i.e., hourly). Based on this physics-based model, we conduct FDD strategies to monitor the inefficiency of building operations.

1.3 Scope

The project aims to demonstrate the effectiveness of the proposed framework, encompassing the following key components:

Comprehensive Case Study

We will conduct an extensive case study that focuses on the simultaneous calibration of multiple parameters, including thermal parameters, control parameters, and schedule fractions. These parameter calibrations will be applied to a high-fidelity physics-based model. The model's output encompasses heating, cooling, and electricity consumption and has been validated using approximately one year's worth of field observations in buildings.

Building Energy Audit

To ensure the reliability of our data and the effectiveness of model calibration, we will perform a thorough audit of the target building. The audit primarily includes energy and waste accounting and the formulation of assessment recommendations.

Building Detection Platform

Furthermore, we will develop a building detection platform for real-time monitoring of the energy usage in the target building and the identification of seven common operational faults that may exist.

1.4 Outline of Report

The report consists of seven chapters. The first chapter is the introduction, which introduces the problems and objectives of this research. The second chapter is the research methods, which provides a detailed introduction to the methods and techniques used in this study. The third chapter is the results, which presents the research findings. The fourth chapter is fault diagnosis and monitoring platform, which details our fault diagnosis methods as well as software. The fifth chapter is the building audit, which analyzes the energy use and energy saving potential of the building in detail. The sixth chapter is student engagement, including poster presentation, building audit, software development and paper presentation. Finally, there are conclusions and references.

2.0 RESEARCH METHODS

2.1 Overview

The research methods can be divided into two main parts (Fig. 1): High-fidelity building and system model, and fault detection & diagnosis and monitoring module. The first part aims to develop a precise physical-based building energy model, which involves data collection, parameter selection, initial building energy modeling, establishing a surrogate model, and calibrating the building energy model. The second part focuses on fault detection and diagnosis, encompassing fault definition and fault monitoring.

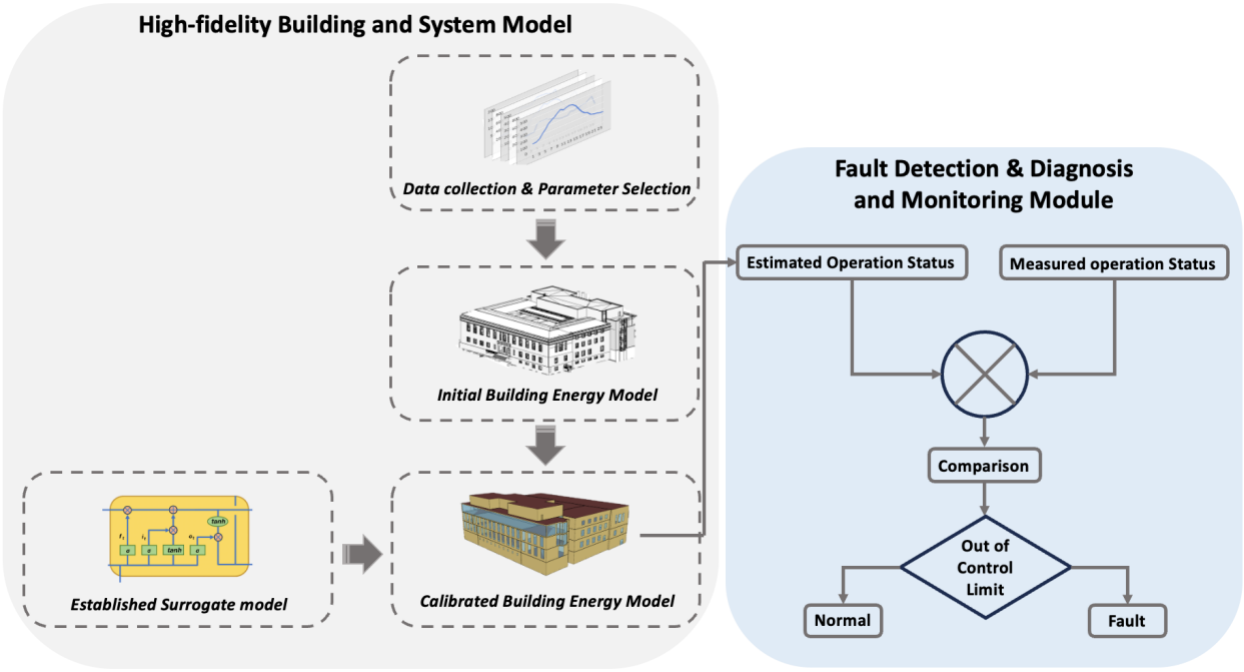

Fig. 1. Physics-modeling-based Approach for HVAC Performance Monitoring

2.2 Data Collecting & Parameter Selection

2.2.1 Description

As depicted in Fig. 2, the facility is an educational facility located at the main campus of the University of Utah. The facility is about 126,000 sqft and consists of a mix of spaces, including lecture halls, student study areas, staff offices, and scientific laboratories. The building employs a

Variable Air Vollum (VAV) system for air conditioning, comprising two Air Handling Units (AHUs). The cooling is supplied by a central plant on the campus, while the heat is generated by four boilers within the building. The facility houses about one hundred employees but facilitates the learning of thousands of students every year. The facility houses about 100 employees on regular 8-hour shifts working Monday through Friday. The labs are used for research and must maintain constant air turnovers because of hazardous chemicals stored in the building. Thus the facility systems always remain active, resulting in annual operating hours of 8760 per year.

2.2.2 Data collection

The calibration process is based on hourly energy consumption data, including heating, cooling, and electricity, collected from the Building Management System (SkySpark) from January to December 2021. There are approximately three months of missing data (mainly in July and August). For a few data gaps due to sensor disconnection, adjacent day types were used to fill in the missing values.

Fig.2. CSC Building.

2.2.3 Parameter selection

There are three types of parameters in building energy models: thermal parameters, control parameters, and schedule fraction. Building thermal parameters can measure the performance of a building, while control parameters can determine whether the building system is in good operation state. Schedule fraction can illustrate the real-time number of occupants and energy usage. In this study, we selected appropriate building thermal performance parameters and control parameters based on sensitivity analysis and research interests. Previous studies have shown a significant

relationship between electricity consumption and schedule parameters [2], [3]. We obtain the schedule fraction parameters by clustering the daily electricity load profile. The daily electricity profile is clustered into two categories, namely workdays and weekends, as shown in Fig. 3.

By normalizing the daily electricity profile, an hourly schedule profile is generated, as shown in Fig. 4. Segmenting the hourly schedule based on similarity enables a reduction in the number of schedule fraction parameters from 24 to 10 for reducing parameters and simplifying the model, as illustrated in Fig. 5. Box plots and quartiles are utilized to determine a more accurate prior range for the schedule fraction.

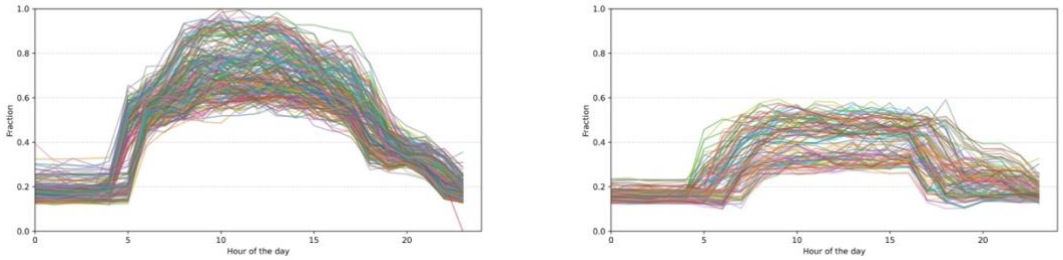

Fig. 3. Electricity consumption clusters (lift: workdays, right: weekends)

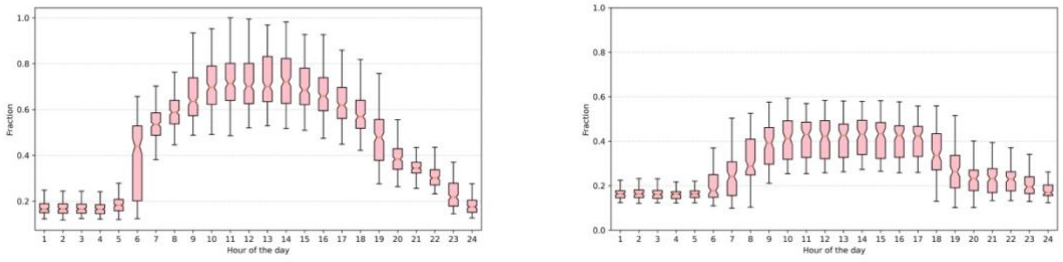

Fig. 4. Hourly schedule (lift: workdays, right: weekends)

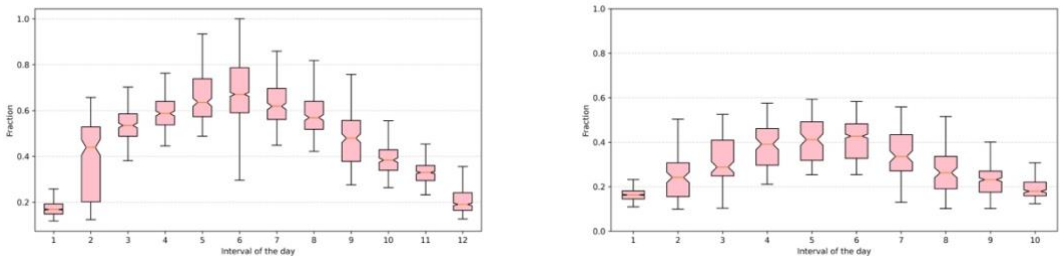

Fig. 5. Interval schedule (lift: workdays, right: weekends)

Table 1. presents the comprehensive list of calibration parameters, amounting to a total of 38 model parameters, covering building thermal properties, building control setpoints, and building operation schedules. All these uncertainties are utilized as prior distributions (triangle distribution) in the Bayesian calibration process.

Table 1. Uncertainty of calibration parameters.

Thermal parameters	Min	Mode	Max	**Control parameters**	Min	Mode	Max	**Schedule parameters**							
								Workdays	Min	Mode	Max	**Weekends**	Min	Mode	Max
Conductivity of wall insulation (W/m·K)	0.03	0.04	0.05	Cooling set-point at occupied hours (℃)	20	24	26	Interval 1	0.1	0.2	0.3	Interval 1	0.1	0.15	0.2
Conductivity of roof insulation (W/m·K)	0.08	0.09	0.10	Cooling set-point at unoccupied hours (℃)	24	26	28	Interval 2	0.1	0.35	0.6	Interval 2	0.1	0.25	0.4
Conductivity of window glass (W/m·K)	0.01	0.015	0.02	Heating set-point at occupied hours (℃)	18	21	24	Interval 3	0.4	0.5	0.6	Interval 3	0.2	0.35	0.5
SHGC	0.3	0.5	0.8	Heating set-point at unoccupied hours (℃)	12	18	20	Interval 4	0.4	0.55	0.7	Interval 4	0.2	0.35	0.5
Electric equipment definition (W/m^2)	5	15	30	Chilled water supply temperature for AHU (℃)	3	6	9	Interval 5	0.5	0.65	0.8	Interval 5	0.3	0.45	0.6
Lights definition (W/m^2)	5	10	15	Supply air temperature of each AHU (℃)	10	14	18	Interval 6	0.5	0.7	0.9	Interval 6	0.3	0.45	0.6
People definition (m^2/person)	5	10	15	Outdoor air flow at occupied hours (1/h)	0	2	4	Interval 7	0.5	0.65	0.8	Interval 7	0.2	0.35	0.5
				Outdoor air flow at unoccupied hours (1/h)	0	1	2	Interval 8	0.4	0.55	0.7	Interval 8	0.1	0.25	0.4

	Hot water peak flow rate (m^3/s)	0	0.0025	0.005	Interval 9	0.3	0.45	0.6	Interval 9	0.1	0.25	0.4
					Interval 10	0.3	0.4	0.5	Interval 10	0.1	0.2	0.3
					Interval 11	0.2	0.3	0.4				
					Interval 12	0.1	0.2	0.3				

2.3 Building Model Calibration

2.3.1 Initial model

A building energy model of the research was constructed using EnergyPlus (version 9.6) (Fig. 6), leveraging the Building Information Model (BIM) (Fig. 7) and adhering to the building design code [4]. The weather data files were provided by White Box Technologies [5]. The outputs of the model correspond to the actual heating, cooling, and electricity consumption of the building, respectively.

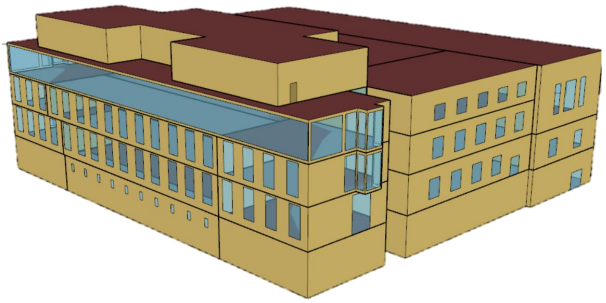

Fig.6. Building energy model in EnergyPlus.

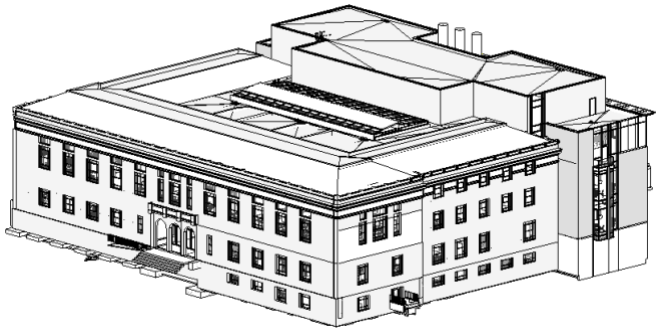

Fig.7. Building information model in REVIT.

2.3.2 High-resolution surrogate model

The surrogate model is an alternative approach that replaces the initial time-consuming simulations, aiming to overcome the computational burden. In this research, we apply LSTM [6] as a high-resolution surrogate model to capture the complex nonlinearity and temporal dependency of building energy model. Long Short-Term Memory (LSTM) is a variant of RNN that is better equipped to retain historical data in memory without experiencing the vanishing gradient problem [7]. LSTM has proven to be effective in memorizing, classifying, processing, and predicting time series data with unknown time lags [8], [9].

In Fig. 8, each LSTM unit has outputs (h) and a cell state (C). At step t, the input (h_{t-1}, C_{t-1}, x_t) consists of the output (h_{t-1}, C_{t-1}) from the previous step $t-1$ and the input parameters (x_t) for step t. By passing through the forgetting gate f_t, updating gate i_t, and output gate o_t, the new unit output h_t and cell state C_t are obtained. This mechanism enables continuous forward propagation and captures long-term dependencies, addressing the correlation and thermal inertia of building thermal processes.

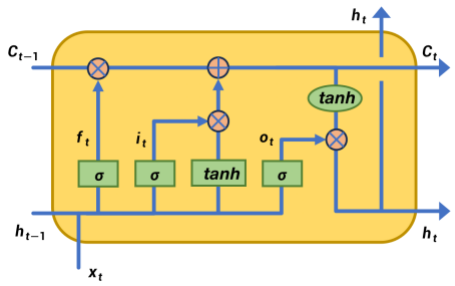

Fig. 8. LSTM cell structure

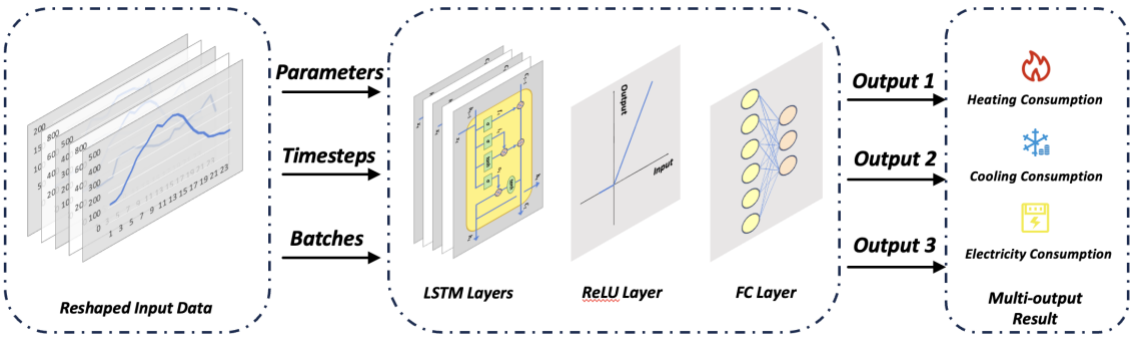

Fig. 9. High-resolution surrogate model framework

The proposed LSTM network architecture, as shown in Fig. 5, consists of an input layer, LSTM layers, a ReLU layer, and a fully connected output (FC) layer. The input layer is derived from the raw dataset through reshaping and splitting, resulting in three dimensions: input size, time step, and batch size. Input size represents the number of input parameters for the model, time step represents the length of each time series data, and batch size represents the total number of time series data. The output layer has three outputs: cooling, heating, and electricity consumption.

This deep network architecture aims to capture the complex nonlinearity of the dynamic thermal processes of buildings while preserving the model's ability to fit building simulations under various parameter settings. As suggested in references [10], [11], a FC layer is typically added after the LSTM layer to map all the predicted sequence to the desired output size. Additionally, we innovatively introduced the ReLU layer after the LSTM layer to enhance the performance and robustness of the model. This is achieved through the function , where negative values are transformed to zero. It should also be noted that the optimal number of LSTM layers needs to be redefined for each unique building case.

A Latin Hypercube sampling technique [12] is employed to generate scenario design points based on the uncertainty of the input parameters. These points are used to simulate hourly energy consumption, resulting in a simulation dataset. The dataset is normalized and used as training data for the surrogate model. A two-layered multi-output LSTM model is fitted as the surrogate model to establish the relationship between the model inputs and the outputs of interest. The LSTM model parameters are specified in Table 2.

Table 2.

LSTM model parameters.

Training data size	140158
Test data size	35040
Input dimension	37
Output dimension	3
Hidden dimension	128
LSTM Layers	2

Epochs	200
Learning rate	0.001

2.3.3 Automated calibration method

Within the framework of KOH Bayesian calibration [13], the relationship between the observation y_i, the true process $\zeta(x_i)$, and the computer simulation model output $\eta(x_i, \theta)$ is described by the Eq. 1.

$$y_i = \zeta(x_i) + e_i = \eta(x_i, \theta) + \delta(x_i) + e_i \quad (1)$$

where e_i represents the observation error for the ith observation and $\delta(x_i)$ is a model inadequacy function independent of the computer simulation output $\eta(x_i, \theta)$. We assume that the e_is are independently distributed as $N(0, \sigma_y^2)$.

For the calibration of building energy models, y_i represents the actual building observations, including cooling, heating, electricity consumption, etc., which can be obtained from the Building Management System (BMS) or meters. $\zeta(x_i)$ represents the true building thermal process, and $\eta(x_i, \theta)$ represents the output of a computer simulation model such as EnergyPlus or Trnsys. x_i denotes the field weather data obtained from the local weather station, and θ represents the model parameters to be calibrated.

A LHS is employed to generate 3220 scenario design points (m=20) based on the uncertainty of the input parameters. These points are used to simulate hourly energy consumption, resulting in a simulation dataset comprising 175200 points with 32 parameters and 3 outputs. A Markov Chain Monte Carlo (MCMC) [14] sampling is conducted with 10,000 runs to explore the posterior distribution, with the first 1000 sample points discarded as burn-in.

2.4 Fault Detection and Diagnosis

2.4.1 Fault model definition

Table 3 summarizes the list of 7 common operation fault models developed in this study.

Table 3. List of fault models considered in this study

Fault Name	Fault Intensity Definition	Fault Intensity Range
Supply air duct leakages	Ratio of the leakage flow relative to supply flow	0 to 0.3
Thermostat measurement bias	Thermostat measurement bias in K	-2.2 to 2.2 K
Dampers stuck at certain position	Ratio of economizer damper at the stuck position (0 = completely closed, 1 = completely open)	0 to 1
Supply air temperature sensor	Biased temperature level in K	-2.2 to 2.2 K
Air handling unit fan motor degradation	Ratio of fan motor efficiency degradation	0 to 0.3
Duct fouling	Reduction in air flow in the duct system at full load condition as a ratio of the design air flow rate	0 to 0.3
Excessive Infiltration	Ratio of excessive infiltration around the building envelope compared to the normal condition	0 to 0.3

- Fault 1: Air duct leakages

Duct leakage can be caused by torn or missing external duct wrap, poor workmanship around duct takeoffs and fittings, disconnected ducts, improperly installed duct mastic, and temperature and pressure cycling. Conditioned air leaking to an unconditioned space in buildings or to the ambient space increases the heating or cooling consumption. The fault intensity is defined as the ratio of the leaked flow relative to the normal airflow.

- Fault 2: Thermostat Measurement Bias

Drift of thermostat temperature sensors over time can lead to increased energy use and/or reduced occupant comfort. the fault model for thermostat measurement bias simulates a biased thermostat by modifying the heating and cooling setpoints assigned to thermal zones. The fault

intensity is defined as the absolute thermostat measurement bias (K), where a positive number means the sensor reading is higher than the true temperature.

- Fault 3: Dampers Stuck at a Fixed Position

Stuck dampers can be caused by seized actuators, broken linkages, control system failures, or the failure of sensors that are used to determine the damper position. In extreme cases, dampers stuck at either 100% open or closed can have a serious impact on system energy consumption or occupant comfort in the space. This fault is implemented by overriding the control algorithm to fix the damper permanently at a user specified value. The fault intensity for this fault is defined as the stuck economizer damper position (0 = fully closed, 1 = fully open).

- Fault 4: Biased Supply Air Sensor

When a sensor drifts and is not regularly calibrated, it causes a bias. Sensor readings often drift from their calibration with age, causing equipment control algorithms to produce outputs that deviate from their intended function. The biased supply air temperature sensor fault is simulated by modifying a setpoint schedule. The fault intensity is defined as the temperature offset (K), where a positive number means that the sensor reading is higher than the true temperature.

- Fault 5: Air Handling Unit Fan Motor Degradation

Fan motor degradation occurs because of bearing and stator winding faults, leading to a decrease in motor efficiency and an increase in overall fan power consumption. The fault model simulates the air handling unit fan motor degradation by modifying the total efficiency of the fan based on the user-defined fault intensity. The fault intensity for this fault is defined as the ratio of fan motor efficiency degradation, with an application range of 0 to 0.3 (30% degradation).

- Fault 6: Duct Fouling

Ducts are fouled by dust that accumulates in the filter and/or fins of heat exchangers in indoor air ducts. The accumulation increases the flow resistance of the air duct and changes the airflow through, and pressure drop across. The fault model simulates the duct fouling by modifying the pressure rise in the fan model based on the user-defined fault intensity. The fault intensity is

defined as the reduction in pressure rise at full load condition as a ratio of the design pressure rise, with an application range of 0 to 0.3 (30% reduction).

- Fault 7: Excessive Infiltration

Excessive infiltration through the building envelope from outside air typically results from cracks in the building envelope and overuse of windows and doors. Infiltration is driven by pressure differences between the building exterior and interior caused by wind and by air buoyancy forces, known commonly as the stack effect. Excessive infiltration can affect thermal comfort, indoor air quality, heating and cooling demand, and the moisture levels of building envelope components, leading to moisture damage. The infiltration through the building envelope can be modeled in EnergyPlus with varying levels of fidelity, from constant infiltration during the entire simulation period, to modulated infiltration in each time step, depending on the ambient conditions (temperature and wind speed). The fault intensity is defined as the ratio of excessive infiltration through the building envelope compared to the normal condition.

3.0 RESULTS

3.1 Parameters Estimation

The calibrated parameters values are presented in Table 4.

Table 4.

Estimated parameters values.

Thermal parameters	Calibrated value	Control parameters	Calibrated value	Schedule parameters			
				Workdays	Calibrated value	Weekends	Calibrated value
Conductivity of wall insulation (W/mK)	0.031	Cooling set-point at occupied hours (℃)	22.22	Interval 1	0.1	Interval 1	0.1
Conductivity of roof insulation (W/mK)	0.08	Cooling set-point at unoccupied hours (℃)	26.67	Interval 2	0.2	Interval 2	0.16
Conductivity of window glass (W/mK)	0.0198	Heating set-point at occupied hours (℃)	20	Interval 3	0.492	Interval 3	0.256
SHGC	0.619	Heating set-point at unoccupied hours (℃)	12.78	Interval 4	0.63	Interval 4	0.45
Electric equipment definition (W/m^2)	20	Chilled water supply temperature for AHU (℃)	5.5	Interval 5	0.73	Interval 5	0.425
Lights definition (W/m^2)	6	Supply air temperature of each AHU (℃)	11.5	Interval 6	0.81	Interval 6	0.485

People definition (m^2/person)	13.5	Outdoor air flow at occupied hours (1/h)	1.05	Interval 7	0.68	Interval 7	0.42
		Outdoor air flow at unoccupied hours (1/h)	0.647	Interval 8	0.64	Interval 8	0.2
		Hot water peak flow rate (m^3/s)	0.001	Interval 9	0.56	Interval 9	0.18
				Interval 10	0.34	Interval 10	0.1
				Interval 11	0.34		
				Interval 12	0.1		

3.2 Model Validation

By calibrating the building energy model using observational data, we obtained the model parameter values under actual operation scenarios (Table 4). Substitute the calibrated parameters into the initial model to obtain the data twin model under actual operation scenarios, which can serve as a benchmark for Fault detection and diagnosis. By validation, the comparison between the observed hourly energy consumption and the simulation outputs of the calibrated model is illustrated in Fig. 6. The simulation results for cooling, heating, and electricity consumption closely align with the field observation data. The corresponding NMBE for heating, cooling, and electricity are 4.5%, -2.9%, and 5.5% respectively, as shown in Table 5. Additionally, the CVRMSE for heating, cooling, and electricity are 23.9%, 28.4%, and 26.9% respectively. It is noteworthy that all types of energy consumption exhibit satisfactory performance and comply with ASHRAE guidelines.

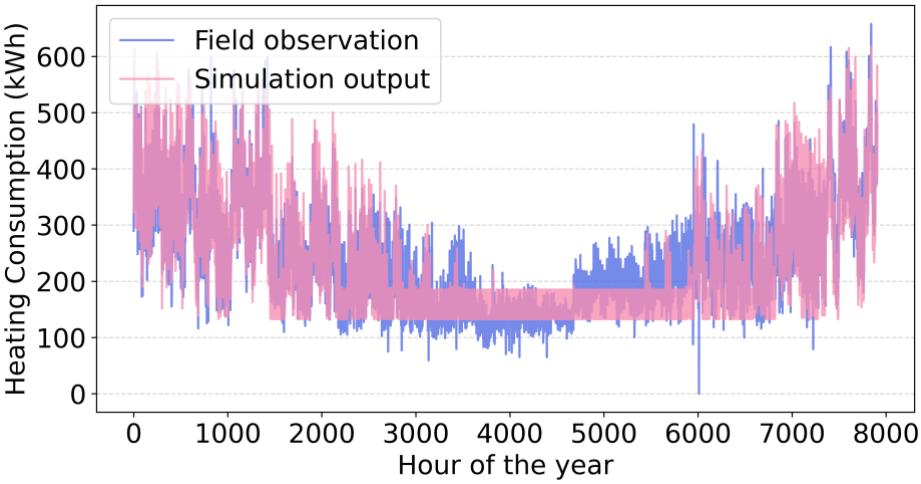

Fig. 10.a. Comparison of heating results.

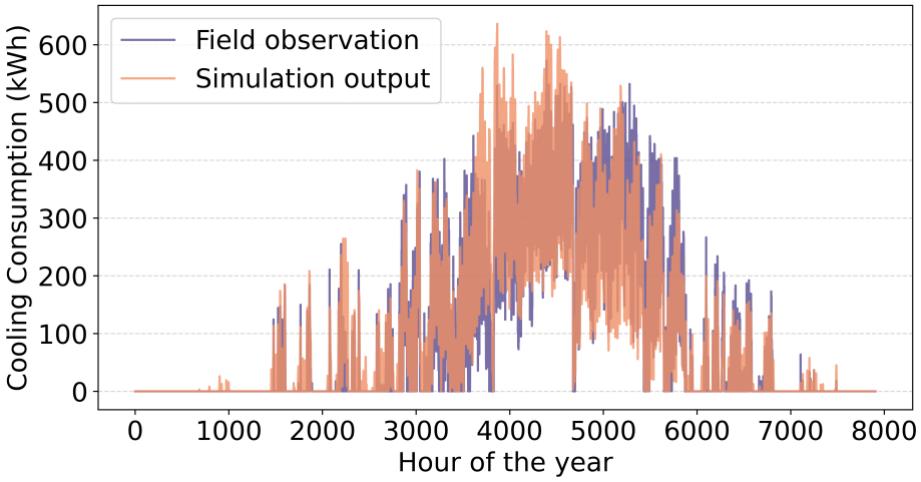

Fig. 10.b. Comparison of cooling results.

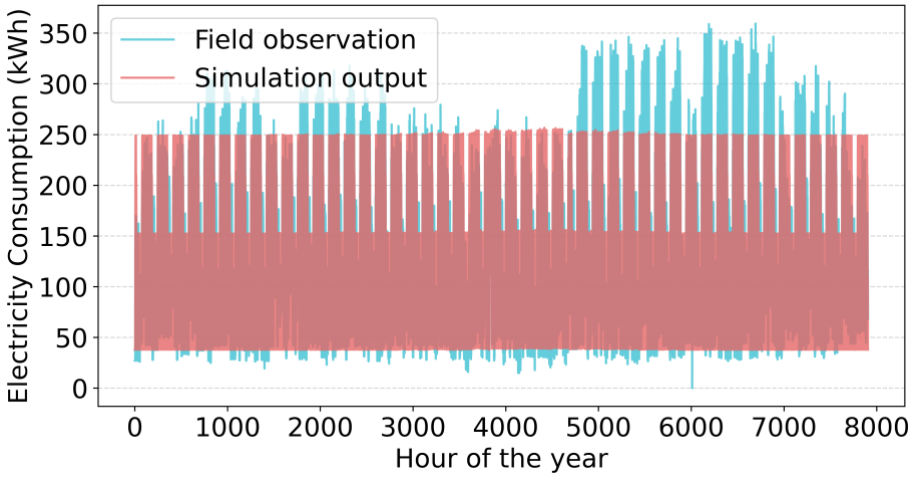

Fig. 10.c. Comparison of electricity results.

Table 5.

RMSE and MBE of calibrated model.

	Heating (kWh)		Cooling (kWh)		Electricity (kWh)	
	NMBE (%)	CVRMSE (%)	NMBE (%)	CVRMSE (%)	NMBE (%)	CVRMSE (%)
Calibrated model	4.5	23.9	-2.9	28.4	5.5	26.9

3.3 Fault Modeling

3.3.1 Air duct leakages

Fig. 11 illustrates a simulation example of air duct leakages in a day (June 1st). The orange solid line represents the actual cooling consumption of the building, the blue solid line represents the simulated cooling consumption of the building without faults, and the blue dashed line represents the simulated cooling consumption of the building under the fault condition. As depicted in the figure, the additional energy consumption by the fault of air duct leakage starts at the first occupied hour (7 am) and reaches its peak at 1 pm. We simulate air duct leakage by increasing the outdoor air flow by 30% to mimic the fault. The results show that the cooling consumption increased by 8.6% in a day.

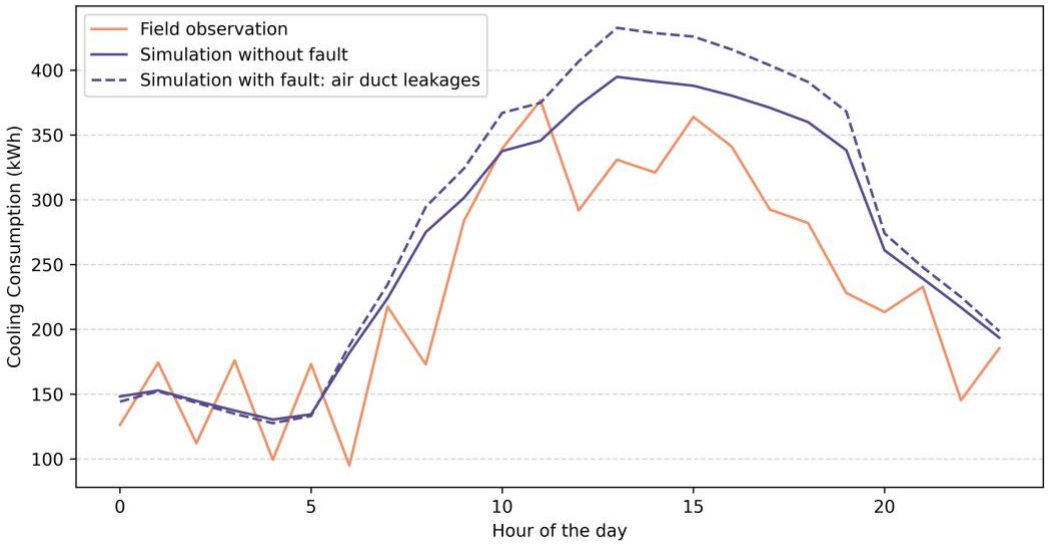

Fig. 11. Simulation example of air duct leakages.

3.3.2 Thermostat measurement bias

Fig. 12 presents a simulation example of thermostat measurement bias during a day. The orange solid line represents the actual cooling consumption of the building, the blue solid line represents the simulated cooling consumption of the building without any faults, and the blue dashed line represents the simulated cooling consumption in the event of a building fault. As shown in the figure, the fault of thermostat measurement bias only occurs during the occupied period, and as the load increases, the consumption caused by the fault also increases. We simulate thermostat measurement bias by reducing the cooling setpoint by 2.2 °C. The results show that the cooling load increased by 16.9% in a day.

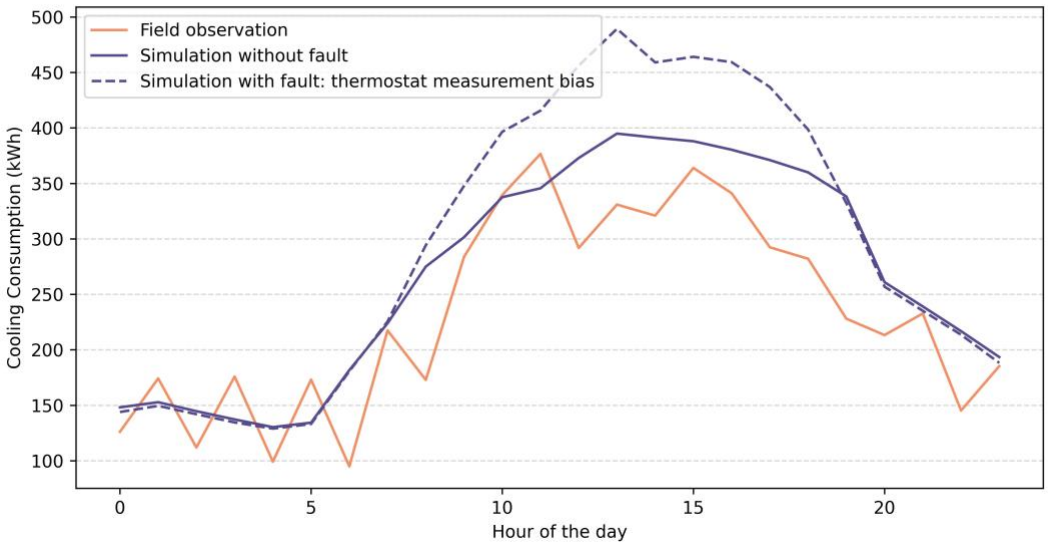

Fig. 12. Simulation example of thermostat measurement bias.

3.3.3 Dampers stuck at a fixed position

Fig. 13 showcases a simulation example of dampers stuck at a fixed position during a day. The orange solid line represents the actual simulated cooling consumption of the building, the blue solid line represents the simulated cooling consumption of the building without faults, and the blue dashed line represents the simulated cooling consumption of the building under the fault condition. As depicted in the figure, the fault of damper stuck only occurs during the occupied period, and the consumption caused by the fault is relatively uniform during that period. In this scenario, the

supply air damper under the fault operation scenario is 30% larger than that under normal operation. The stuck damper results in a higher mixed-air temperature compared to the mixed-air temperature of the normally operated condition. Since this mixed-air temperature must be cooled down to the supply air temperature setpoint, the faulted case results in an additional 4.9% cooling consumption during a day.

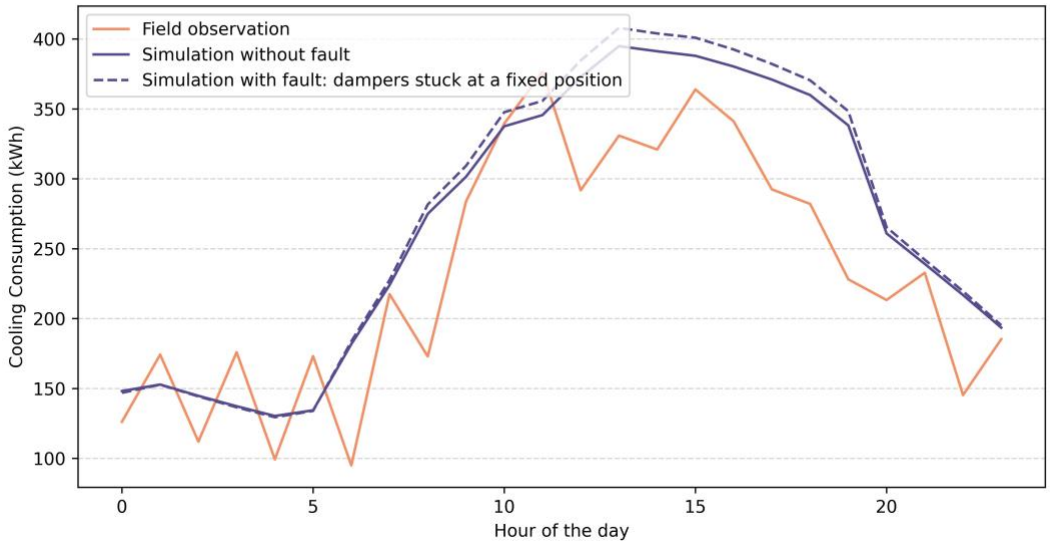

Fig. 13. Simulation example of dampers stuck at a fixed position.

3.3.4 Biased supply air sensor

Fig. 14 demonstrates a simulation example of biased supply air sensor fault during a day. The orange solid line represents the actual cooling consumption of the building, the blue solid line represents the simulated cooling consumption of the building without faults, and the blue dashed line represents the simulated cooling consumption of the building under the fault condition. From the figure, it can be observed that the supply sensor bias fault occurs throughout the day and to the same extent. To mimic this condition, we increased the supply air temperature setpoint by 3°C, which simulates a scenario where the supply air temperature sensor reads 3°C lower than the true value. As a result, the additional cooling consumption amounts to 15.0% because the HVAC system requires a lower supply air temperature.

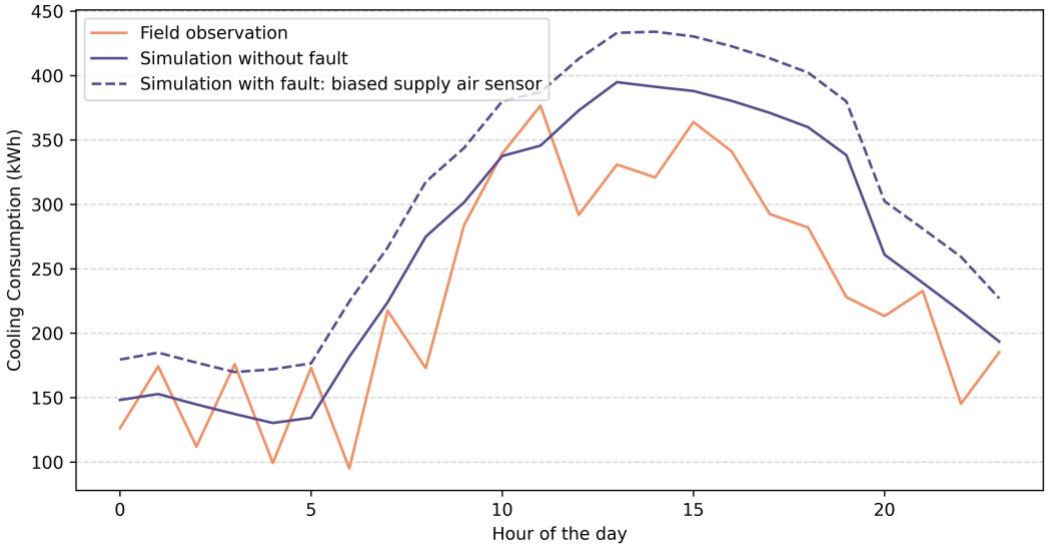

Fig. 14. Simulation example of biased supply air sensor.

3.3.5 Fan motor degradation

Fig. 15 depicts a simulation example of fan motor degradation fault during a day. The orange solid line represents the actual simulated cooling consumption of the building, the blue solid line represents the simulated cooling consumption of the building without faults, and the blue dashed line represents the simulated cooling consumption of the building under the fault condition. As shown in the figure, the fault of fan motor degradation occurs throughout the day, resulting in the same additional consumption. We simulate the degradation by reducing the total efficiency of the fan by 30%. Although the fan is only a device in the subsystem and has a relatively small impact on the cooling consumption, the fault persists throughout the day, leading to an additional 7.2% of cooling consumption.

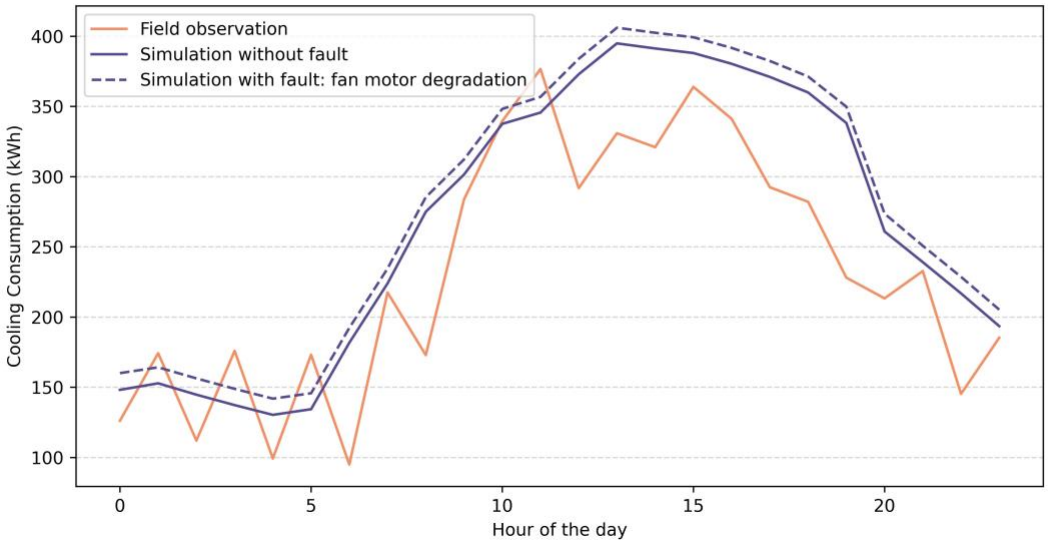

Fig. 15. Simulation example of fan motor degradation.

3.3.6 Duck fouling

Fig. 16 displays a simulation example of air duct fouling during a day. The orange solid line represents the actual simulated cooling consumption of the building, the blue solid line represents the simulated cooling consumption of the building without faults, and the blue dashed line represents the simulated cooling consumption of the building under the fault condition. Regarding duct fouling, the fault occurs throughout the day with the same trend. Although air duct fouling has a relatively small impact on cooling load, it persists throughout the day, resulting in an additional 4% of cooling consumption.

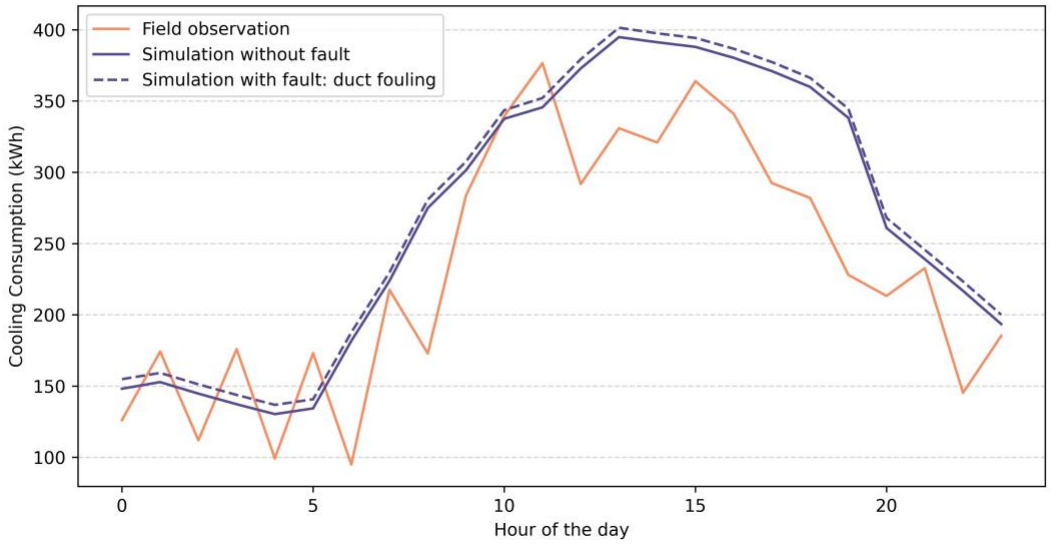

Fig. 16. Simulation example of duck fouling.

3.3.7 Excessive infiltration

Fig. 17 exhibits a simulation example of excessive infiltration during a day. The orange solid line represents the actual simulated cooling consumption of the building, the blue solid line represents the simulated cooling consumption of the building without faults, and the blue dashed line represents the simulated cooling consumption of the building under the fault condition. As shown in the figure, excessive infiltration occurs when the building infiltration is increased by 30%, simulating a condition where the building experiences excessive infiltration. These excessive infiltration events mainly occur during the occupied period, and their additional energy consumption increases with increasing load, reaching a peak at 1 pm. Consequently, there is an additional 7.7% cooling consumption.

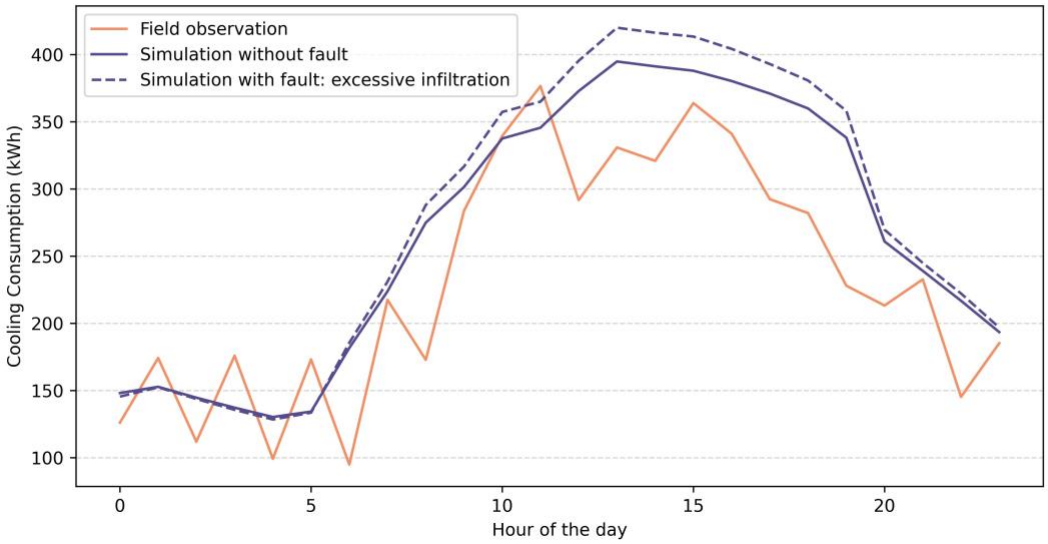

Fig. 17. Simulation example of excessive infiltration.

4.0 Fault Detection & Diagnosis, and Monitoring Platform

4.1 Summary

The platform incorporates a calibrated physical building energy model, acting as a digital twin, which connects to real-time building and system operation information queried from the SQL database linked with SkySpark and building automation systems. Through continuous real-time monitoring, the platform can detect deviations in system operation performance by comparing the digital twin's estimations of building dynamics with actual measurements. The building facility manager can log in to the platform's software and access all alarms or decisions generated from the continuous monitoring process (Fig. 18).

4.2 Introduction to Software Functions

The software consists of five main modules, as shown in Figure 19: Offline Data Comparison, Building Supervision, Model Prediction, Operation Evaluation, and Fault Report. The Data Comparison module facilitates rapid energy consumption data analysis during offline processes, allowing operational personnel to efficiently compare and calculate deviations between the real-time system operation and the desired ideal operation. This feature is designed for use by maintenance personnel in offline scenarios, offering a degree of flexibility in its application (Fig. 20). The Building Energy Monitoring module displays real-time energy consumption and trends within the building throughout the day, enabling operators and managers to understand the building's current operation (Fig. 21). The Building Energy Prediction module provides real-time energy consumption predictions based on the digital twin, offering the ideal energy consumption of building systems under normal operating conditions, and serving as a reliable basis for fault diagnosis strategies (Fig. 22). The Operation Fault Evaluation module assesses the energy consumption of systems within the building from various dimensions and scales, calculating the potential energy-saving opportunities under the current operating scenario (Fig. 23). The Fault Reporting module utilizes the expert rule library provided, comparing the current building operating scenario with known fault in the library to identify potential operational faults. This allows building managers and operators to carry out fault inspection work efficiently (Fig. 24). The various functions of the software are closely connected, and data will be interactive. Real-

time supervision and model prediction data of buildings serve as input data for fault diagnosis, and the diagnostic results will be issued as a fault report.

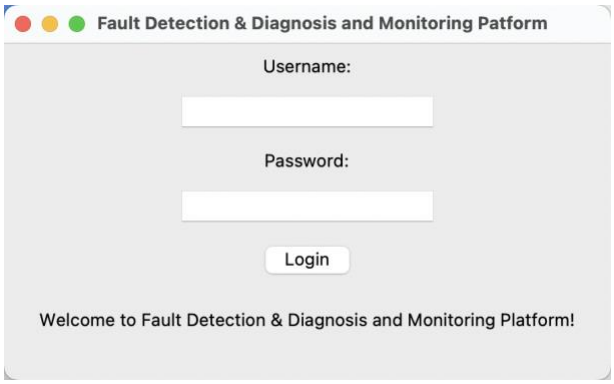

Fig. 18. Login screen of the software.

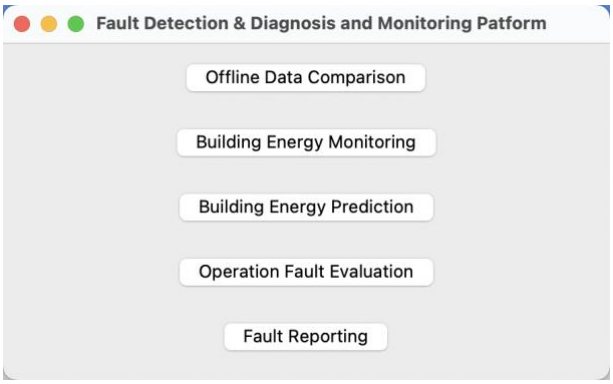

Fig. 19. Main screen of the software.

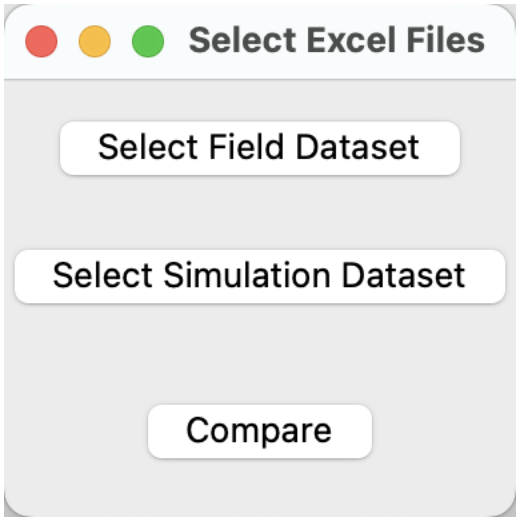

Fig. 20. Offline data comparison.

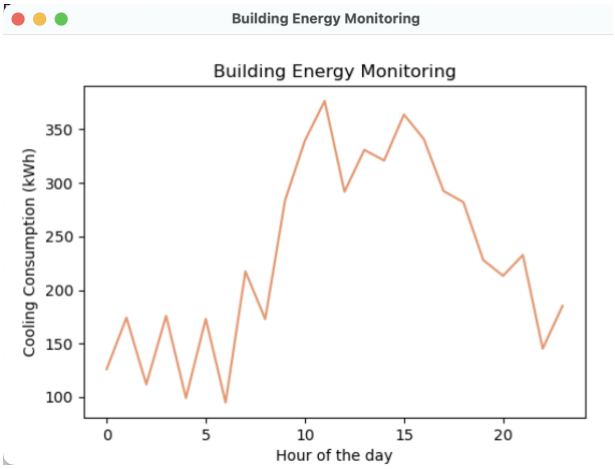

Fig. 21. Building monitoring screen.

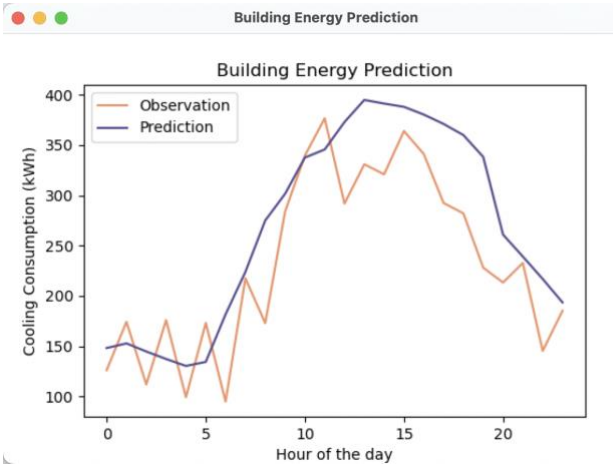

Fig. 22. Model Prediction screen.

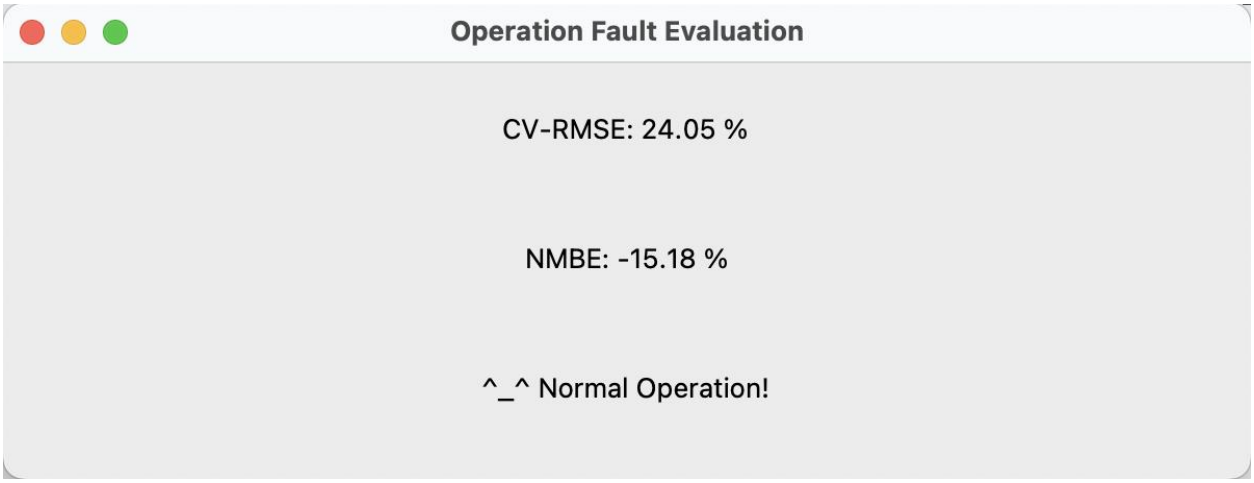

Fig. 23. Operation evaluation screen.

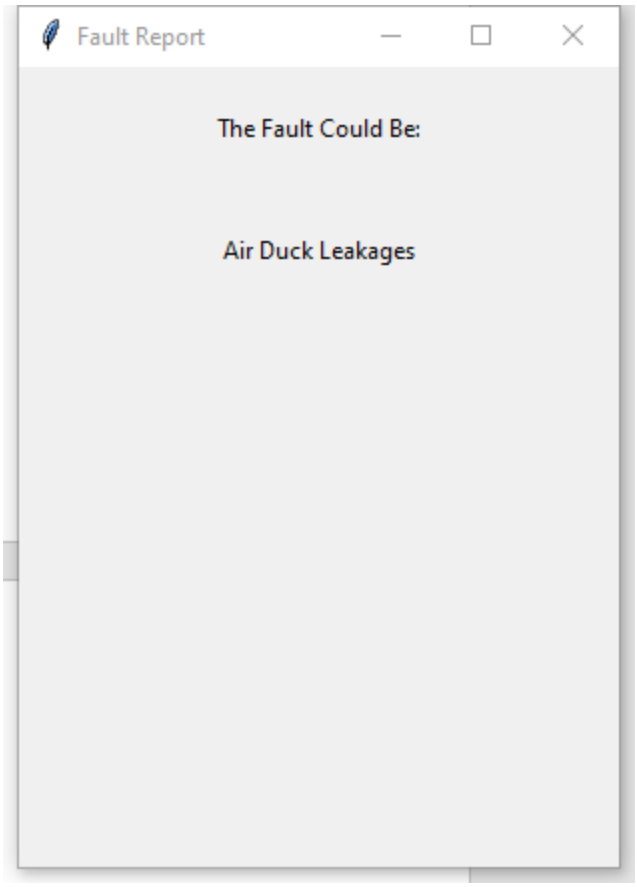

Fig. 24. Fault Report screen.

5.0 BUILDING AUDITING

5.1 Auditing Description

The facility is an educational facility located at an institution of higher education. The facility is about 126,000 sq ft and consists of a mix of spaces, including lecture halls, student study areas, staff offices, and scientific laboratories. The audit process begins with a meeting of the audit team to discuss specific details and various issues during the audit. Next, the audit team began their site survey work. First, they scrutinized the operation of pumps and piping in the mechanical room to ensure that these critical components were functioning properly. The audit team then traveled to several rooms to inspect the air conditioning and cooling systems to assess indoor comfort and ensure that the indoor environment met comfort standards while maximizing energy efficiency. The audit team then moved to the lighting control room to assess the status of the lighting fixtures in each room to identify any abnormal lighting conditions. Finally, the audit team arrived at the boiler room on the top floor of the building to assess the condition of the hot water supply and heating systems. The purpose of this assessment was to verify the proper functioning of these systems and also to consider potential opportunities to improve energy efficiency.

The following outlines the facility's major energy-consuming equipment concerning its process. After concluding an energy assessment of the facility, the team has determined that these systems are key contributors to the facility's energy consumption. Although some of the equipment mentioned may not be included in the following recommendations, it is important that this equipment is considered in current and future energy management.

- 30 hp air compressor
- Vacuum pumps
- 4 condensing boilers
- 2 domestic hot water heaters
- Air handling units

5.2 Energy Accounting

An essential component of energy management programs is a detailed account of all resource consumption and the associated cost. This is done by monitoring temporal trends in consumption and supporting long-term energy goals. Taking advantage of available resources and tools with long-term energy goals is an important part of successful energy management programs and can yield significant short and long-term cost benefits. This section provides an overview of the energy accounting data used in this report. The energy data used in this report was sourced directly from facility records. The energy data provided in electric, natural gas, and water bills were reduced to simplify the analysis presentation of this report. Table 6 shows the common conversion factors used in an energy analysis.

Table 6. Common energy conversion factors.

General	
1 MMBtu	1,000,000 British thermal unit (Btu)
Electricity	
1 kWh	3,413 Btu
1 MMBtu	293 kilowatt-hours (kWh)
1 HP (electric)	0.746 (kW)
1 kW	1.314 HP (electric)
Nature Gas	
1 therm (THM)	100,000 Btu
1 deca-therm	10 therms = 1,000,000 Btu = 1 MMBtu

The facility's electrical provider is Rocky Mountain Power. The assessment team was provided with a BAS system that measured and recorded all meters to the building. Annually the facility uses 1,322,8019 kWh of electricity at a rate of $.0737 per kWh for a total of $97,490 spent in electricity each year.

The facility purchases natural gas from Dominion Energy on a Transport Service rate schedule. The meters measured twelve months of natural gas usage. From the facility, the weighted

average price is $5.59 per MMBtu. During the twelve-month interval, the facility consumed 8057 MMBtu of natural gas, corresponding to a total of $45,043.

This facility purchases chilled water from a central campus system. Ituses chilled water in two ways; there is a process loop that cools machinery in the building, and a second sub-process loop that brings chilled water to AHUs and chilled seams. The price for chilled water is $9.180 per MMBtu. The facility has an annual usage of 4229 MMBtu for a total of $38,822.

The total annual utility cost for the facility is $181,335. Fig. 25 shows a breakdown of this cost by the utility. A summary of the facility's annual electricity and natural gas usage, along with the facility's rates for electricity and natural gas, are found in Table 7.

Table 7. Total annual utility summary.

Utility	Total Usage	Units	Rate	Units	Total Cost
Electricity	1,322,801	kWh	0.0737	$/kwh	$97,490
Natural Gas	8,057	MMBtu	5.59	$/MMBtu	$45,043
Chilled Water	4,229	MMBtu	9.18	$/MMBtu	$38,822

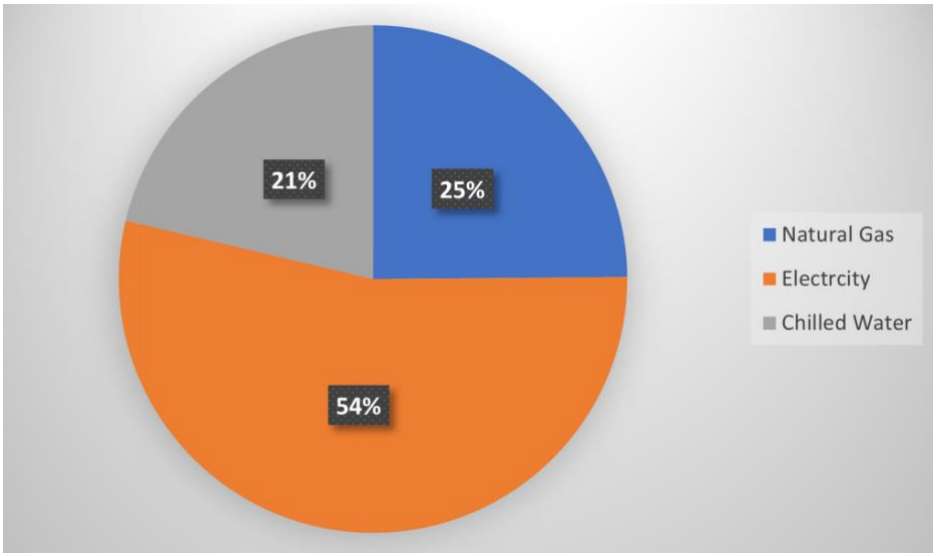

Fig. 25. Utility cost shares by type.

5.3 Assessment Recommendations

5.3.1 AR NO.1: Turn Off Boilers in the Summer

Summary

It is recommended to turn off the four condensing boilers in the summer. In the summer of 2022 they ran unnecessarily, wasting natural gas. Cost and energy savings of this recommendation are shown below.

Table 8. Cost and energy savings.

Estimated Natural Gas Savings [MMBtu/year]	1,950
Estimated Cost Savings [$/year]	$10,910
Estimated Implementation Cost [$]	$800
Estimated Payback Period [years]	0.1

Background and Current Practice

The facility‘s building management system (BMS) logs the natural gas energy rate used by the boilers and the chilled water energy rate used by the air-handling units (AHUs). Fig. 26 shows the natural gas and chilled water energy rate for the summer of 2022. As shown in Figure 4.1, the AHUs use chilled water from June to August (with use before and after this). Natural gas is also being used until August 4th, 2022, when the boilers are turned off briefly until August 15th, 2022. While there are times of the year when both heating and cooling will be necessary to keep the building at a comfortable temperature throughout the day, during the hottest parts of the year, the boilers shouldn’t be necessary at all.

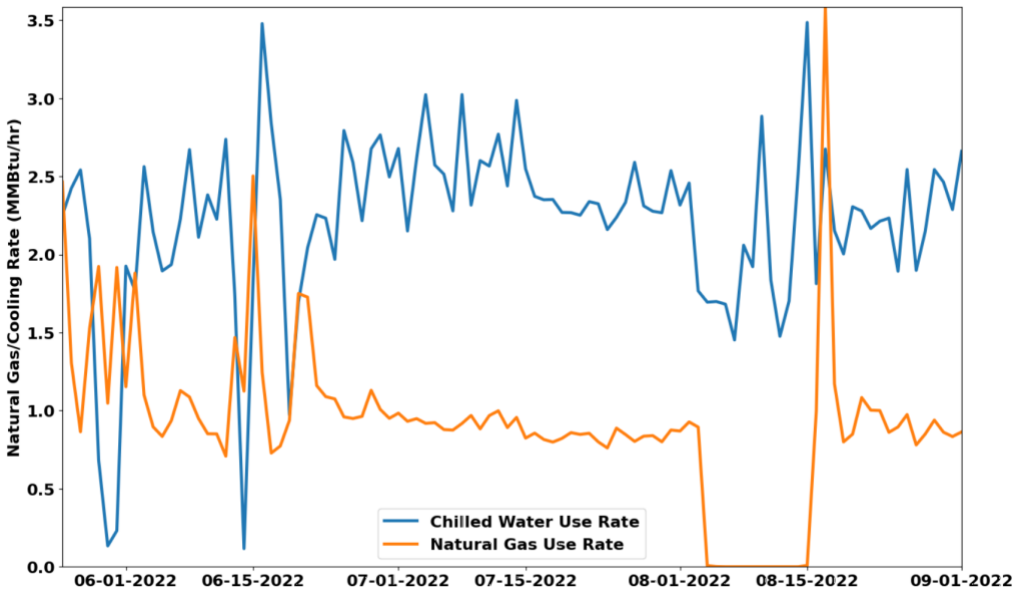

Fig. 26. Logged data from the summer of 2022. The plot shows the natural gas rate from the boilers and the chilled water energy rate in the AHUs.

Anticipated Savings

Natural gas savings are found by calculating the total 2022 natural gas use of the boilers collected by the BMS from June through the end of August. This totals 1,951 MMBtu/yr and $10,905/yr of savings. The data is taken from the BAS monitoring system.

Assumptions

• Occupants will be okay with some colder mornings in the building that may happen in early June or on unseasonable cold summer days.

• Data from June – August 2022 is representative of future summer use.

Implementation Costs

Implementation costs will be in-house labor putting the boilers into a summer off-state at the beginning of June and then putting the boilers back into operation at the end of August. It is assumed this will take 8 hours of labor for both days with an in-house labor rate of $50/hr. Total implementation cost amounts to $800.

5.3.2 AR No. 2: Turn off Chilled Water to AHU in Winter

Summary

It is recommended to locate why the sub-loop to the AHU is running chilled water during the winter and take the necessary actions to correct it. During the winter of 2022-2023, the sub-process loop to the AHU and the chilled beams provided cooling unnecessarily. Cost and energy savings of this recommendation are shown below.

Table 9. Cost and energy savings.

Estimated Chilled Water Savings [MMBtu/year]	344
Estimated Cost Savings [$/year]	$3,162
Estimated Implementation Cost [$]	$2,000
Estimated Payback Period [years]	0.6

Background and Current Practice

The facility‘s building management system (BMS) logs the flow rate of the sub-loop of chilled water to the AHU and the chilled beams in addition to the supply and return temperature of chilled water in this sub-loop. Currently, there is a constant flow of 13 gal/min during the winter, with an average temperature change in the water of 16.05 degrees. The facility usage data from the BAS system is shown in Figure 27. As can be seen in Fig. 27, the AHUs are using chilled water September to April when the building is also using natural gas to warm up air in the AHU. During the winter months, there is a baseline flow of 13.0 gal/min of CW to this sub-loop, while there is no need for chilled water in the winter.

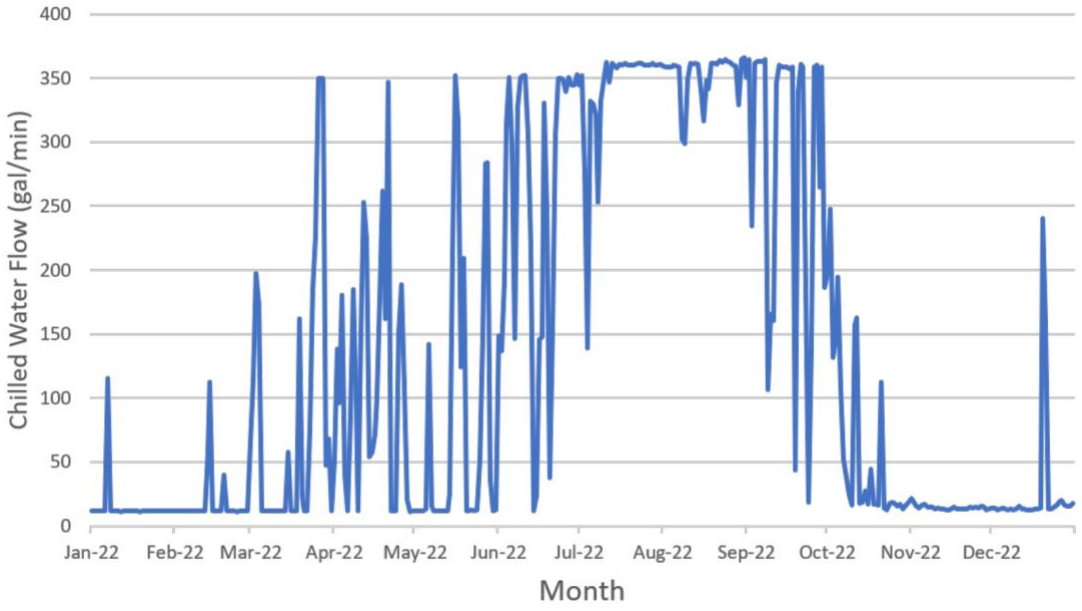

Fig.27. Chilled water usage to the AHUs for one year. Data taken from the BAS system.

Anticipated Savings

Using the baseline flow of 13.0 gal/min obtained using the logged data, and the average ΔT in the supply and return temperature of the CW during the winter which is 16.05 °F. Using these two numbers it was found that the average loss is 104,000 btu/hr. There are 138 days where the CW was run during the winter (warm days excluded). The cost of 1 MMBtu of CW at this facility is $9.18.

$$Energy\ Usage\ \left[\frac{MMBtu}{hr}\right] * Run\ Time\ \left[\frac{hr}{day}\right] * Total\ Days = Energy\ Used\ [MMBtu]$$

$$0.104\ MMBtu * 24hr * 183\ days = 344.4\ MMBtu$$

$$344.4\ MMBtu * 9.18\left[\frac{\$}{MMBtu}\right] = \$3{,}162 MMBtu\ per\ year$$

Assumptions

- All meters are well calibrated, and CW is flowing in the sub-loop during winter months.
- Data from September - April 2022-2023 is representative of future use.

Implementation Costs

Implementation costs is estimated to be a week of internal labor to find out how to turn off CW to the AHU during the winter. One week of internal labor is estimated at $50/hr. This brings the total implementation cost to $2,000.

5.3.3 AR No. 3: Optimize Boiler Temperature Controls

Summary

It is recommended to optimize the condensing boiler temperature controls in various ways. First, the supply temperature setpoint should be lowered. Next, the water flow rate through the condensing boilers and through the air handling units (AHUs) should be lowered. This will increase the change in temperature of water across the AHUs, lowering the return water temperature to the condensing boilers. Condensing boilers are more efficient with lower return water temperatures, saving natural gas. Cost and energy savings of this recommendation are shown below.

Table 10. Cost and energy savings.

Estimated Natural Gas Savings [MMBtu/year]	370
Estimated Cost Savings [$/year]	$2090
Estimated Implementation Cost [$]	$ 2000
Estimated Payback Period [years]	1

Background and Current Practice

The facility has four condensing boilers that supply hot water for the AHUs for space heating. Condensing boilers operate on the principle of recovering latent heat from water in the boiler combustion gas, increasing their combustion efficiency. In order to condense out the water in the combustion gas, the temperature into the boilers (the return water temperature) needs to be below the dew point of the combustion gas.

Currently, the condensing boilers operate with an average return water temperature of 161.9 ◦F and average supply temperature of 167.9 °F. This is found from the most recent year of data collected from the building management system (BMS) for when any one boiler is running. The hot water supply temperature setpoint varies from 150 °F to 180 °F depending on the outside

air temperature from information from site personnel. A plot of the return water temperature and supply temperature from the boilers is shown in Fig. 28.

The efficiency of all the boilers was calculated by finding the thermal heat given to the hot water using the boiler water flow rate and the temperature difference across the boilers throughout the year. Then the logged natural gas energy rate for the boilers was used to calculate a boiler efficiency of 92.8%.

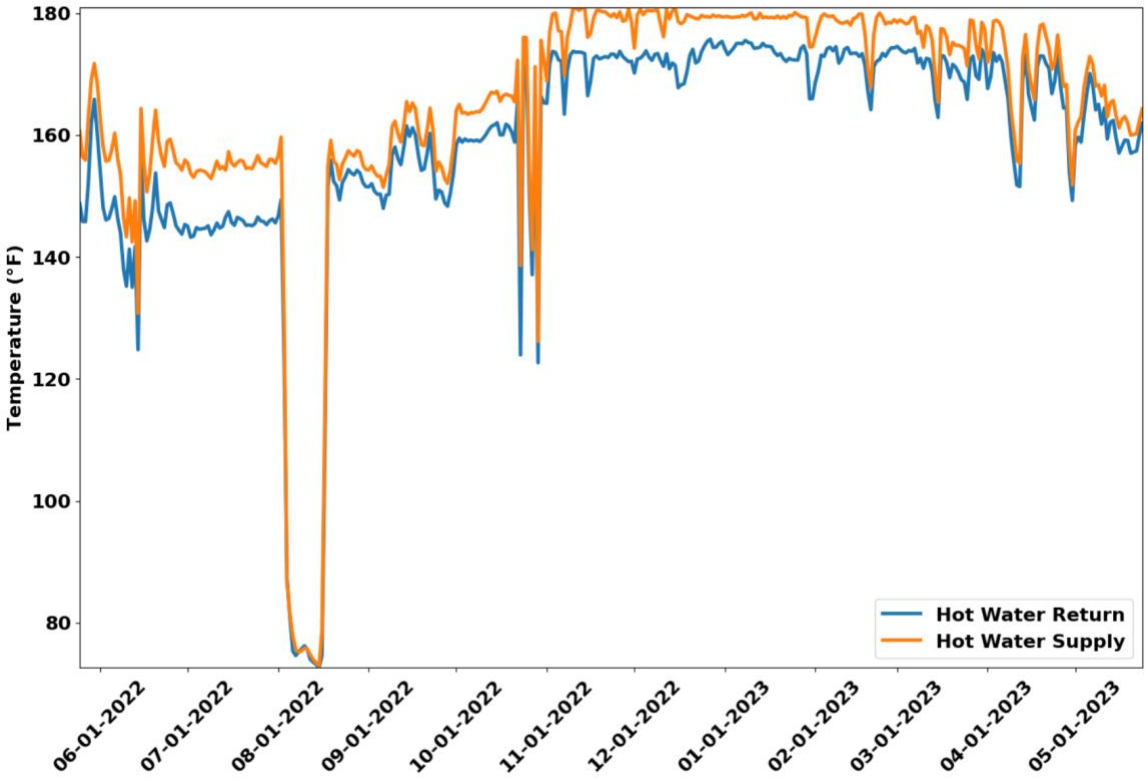

Fig. 28. Boiler supply and return water temperature.

The boilers mainly run in a low fire mode. While running, the boilers' average firing rates are summarized in the table below using the most recent year's worth of data collected from the BMS.

Table 11. Boiler average firing % while running.

Boiler 1	Boiler 2	Boiler 3	Boiler 4
25.1%	29.5%	32.9%	24.0%

Anticipated Savings

Anticipated savings come from increasing the efficiency of the condensing boilers. A plot showing boiler efficiency vs. return water temperature with different firing rates is shown in Fig. 29. It should be noted that this is an example plot and not necessarily representative of the boilers that the facility has.

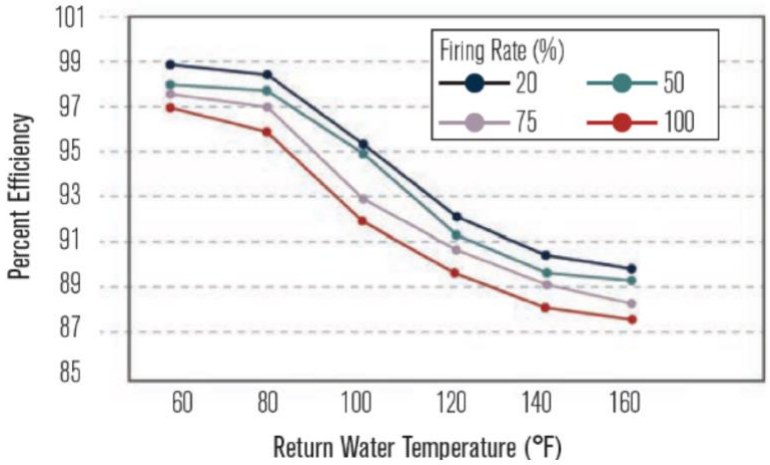

Fig. 29. Firing rate efficiency.

From the plot above, it can be seen that lowering the hot water return temperature can significantly increase the efficiency of the boilers. The assessment team estimates that the overall boiler efficiency can be raised to 95%, effectively lowering the amount of natural gas needed for the same amount of thermal heating. This amounts to 374 MMBtu/yr of natural gas savings totaling $2,091/yr.

Assumptions

• The lower temperatures to the AHUs will not significantly affect heat transfer performance, and they will still be able to provide the necessary heating for the building.

• The condensing boilers can accommodate a higher temperature increase with a lower flowrate per their manual.

• The firing rate of the boilers will remain around the same as the averages in Table 10 with the recommendation implemented.

Implementation Costs

Implementation costs will be in-house labor changing the controls and monitoring the system to make sure it is working correctly. It is assumed this will take 40 hours of labor with an in-house labor rate of $50/hr. Total implementation cost amounts to $2,000.

6.0 STUDENT ENGAGEMENT

Summary

Student engagement in this project encompassed three key areas: participation in research seminar and poster presentation, involvement in the energy audit process, development of modeling software, and publication of paper. The project featured the active participation of two PhD students from the Department of Civil Engineering, as well as one PhD student and one undergrad students from Department of Chemical Engineering.

6.1 Research Symposium and Poster Presentation

This project encompassed a captivating academic symposium, offering all participants an unforgettable scholarly feast. During this symposium, students and scholars from diverse fields and different schools converged to explore the latest developments and achievements within their respective research domains.

Specifically, one PhD student from the Department of Civil Engineering presented this research project through a poster presentation at the symposium, sharing our research direction and outcomes with the attendees (Fig. 30 shows the poster). Scholars from various disciplines gathered at the symposium, providing a platform for interdisciplinary exchange. Valuable advice and feedback were received from scholars of different fields, profoundly impacting the research direction. The experience exposed us to the diversity and richness of the academic world, fostering a deeper understanding of interdisciplinary fusion and the boundless possibilities of knowledge.

During the conference, we had the opportunity to relish delightful beverages and food, adding a pleasant ambiance to the moments of relaxation and informal conversation. In this relaxed setting, we eagerly shared our respective research areas and methodologies. This mutually inspiring exchange not only broadened our academic horizons but also encouraged our team to contemplate how to incorporate ideas from other fields into my research, thereby fostering the creation of more innovative and distinctive outcomes. In sum, this academic seminar provided our team with a precious opportunity, propelling us to take a firmer stride on the path of academic exploration.

Bayesian calibration of campus building energy model for sustainability

Gang Jiang, Jianli Chen* (jianli.chen@utah.edu)

Department of Civil and Environmental Engineering, University of Utah, Salt Lake City, UT 84112

THE UNIVERSITY OF UTAH

GLOBAL CHANGE & SUSTAINABILITY CENTER

Introduction

- Buildings account for 36% of global energy consumption and 19% of greenhouse gas emissions. To predict building energy use and enhance the sustainability, it is critical to obtain an accurate building energy model (BEM).
- Calibration is for bridge the gap between the BEM and the actual building due to uncertainties such as weather fluctuation and human behaviors.
- We calibrate model of a campus building located in University of Utah (Crocker Science Center). The calibration approach is Bayesian calibration, which use Bayesian inference to predict parameters and analyze uncertainties.
- A well calibrated BEM can use for building retrofit, fault diagnosis and detection (FDD), grid-interactive efficient building (GEB), model predict control (MPC), and demand response (DR) to enhance building sustainability.

Initial building energy model

- The initial computer simulation model was constructed by Energy Plus software in conjunction with the building design information.
- The model input are weather information (e.g., temperature and humidity), building information (e.g., construction materials and design drawings), and building system information (e.g., HVAC system schedule, lighting schedule, and occupant behaviors).
- The model output are heating consumption, cooling consumption , electricity use and indoor environment.

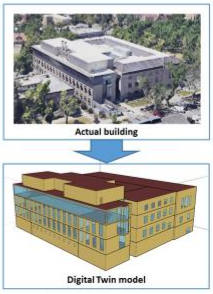

Fig. 1. Initial model workflow

Data collect & Parameter selection

- The building operation data come from building management system. we used 9 months of data from 2021; the other three months were missing.
- We use Latin hypercube sampling (LHS) to sample the parameter range and obtain 200 sets of simulation runs with different parameter combinations as the computer simulation data preparation for conducting model calibration.
- A critical step before calibrating a BEM is to conduct a sensitivity analysis and uncertainty quantification to identify the most influential uncertain model parameters and their ranges. The uncertain parameters in the model and their ranges are listed in Table 1.

Model parameters	Min	Max
Electrical equipment power density (W/m^2)	5	30
Lighting power density (W/m^2)	5	30
Occupancy density (m^2/person)	5	30
Infiltration (m^3/s)	0	0.01
Outdoor air flow rate (m^3/s)	0	0.3
Heat water use (m^3/s)	0	0.002

Table 1. Parameters and their ranges

Bayesian calibration approach

The proposed approach uses Bayesian inference to model the relationship between field observations $\boldsymbol{y}$ and the output of the computer simulations $\boldsymbol{\eta}$, by explicitly accounting for parameter uncertainties, model discrepancy, and observation error (Eq. 1).

$$\boldsymbol{y}(\boldsymbol{x}) = \boldsymbol{\eta}(\boldsymbol{x}, \boldsymbol{t}) + \boldsymbol{\delta}(\boldsymbol{x}) + \boldsymbol{\epsilon} \qquad (1)$$

Where: $\boldsymbol{x}$ is the field observations and computer simulations input (e.g., outdoor dry-bulb temperature and relative humidity).

$\boldsymbol{t}$ is the true but unknown values of the calibration parameters.

$\boldsymbol{t^*}$ is the value of parameters for each simulation.

$\boldsymbol{\delta(x)}$ is the model bias.

$\boldsymbol{\epsilon}$ is the observation bias.

- The first step to calibrating a BEM is to combine field and simulation data in surrogate (Gaussian process) model.
- Rapid data generation using the surrogate model for Bayesian inference.
- Posterior distributions are obtained by Markov chain Monte Carlo(MCMC) sampling.
- Using optimal parameter calibrate BEM model.
- Checking the calibrated model result and

Optimal parameters value	
Electrical equipment power density (W/m^2)	12
Lighting power density (W/m^2)	18
Occupancy density (m^2/person)	15
Infiltration (m^3/s)	0.0085
Outdoor air flow rate (m^3/s)	0.2
Heat water use (m^3/s)	0.00115

Table 2. Optimal parameters value

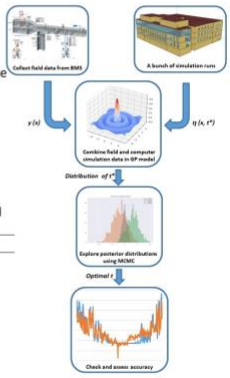

Fig. 2. Bayesian calibration workflow

Posterior parameter distributions

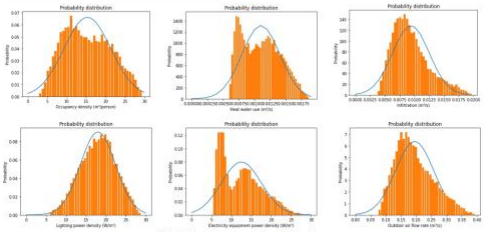

Fig. 3. Posterior parameter distributions

We use the MCMC algorithm for sampling to obtain the posterior distribution of the parameters and obtain the optimal BEM parameters. The posterior parameters distribution are listed in Figure 3.

Validation & Conclusion

- The 3 output results all below the threshold (15%) by the ASHRAE standard for monthly energy data. (Table. 3)
- Bayesian calibration quantifies the impact of uncertainty on parameter calibration based on posterior distributions, which can provide more reliable parameter selection
- A multi-output model calibration approach will yield somewhat poorer results than a single output, but due to the coupling between building systems, a multi-output calibration model will yield a more robust baseline model and more reflective calibration results.

Performance metrics of calibration	
	CV-RMSE
Heating consumption	10%
Cooling consumption	14%
Electricity use	7%
Overall	10.33%

Table 3. Calibration performance

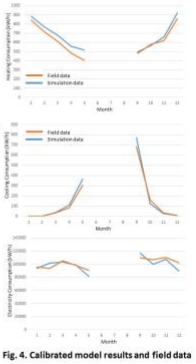

Fig. 4. Calibrated model results and field data

Acknowledgement

Acknowledge SEED2SOIL and GCSC support in any publications or presentations with the statement "Funding has been provided by the University of Utah's SEED2SOIL program with the support the Global Change and Sustainability Center."

Fig. 30. Poster presented at the symposium.

6.2 On-Site Energy Audit

This project also entails an on-site energy audit of the Crocker Science Center, with participation from one undergraduate student and two PhD students. This on-site audit not only helped them apply what they learned in class to a real-world situation, but also enhanced their skills in data collection, energy system analysis, engineering calculations, and formal report writing.

First, the students held a meeting with the organizers where they discussed the specifics of the audit we needed to conduct and the various issues that needed to be considered. The students then traveled to the mechanical room to take a closer look at the working condition of the pumps and pipes. The purpose of this step was to ensure that these critical pieces of equipment were functioning properly and if there were any potential issues. Next, the student team traveled to several rooms and inspected the air conditioning and cooling status of the rooms to determine if there were any indoor comfort issues. The focus of this session was to ensure that the indoor environment was comfortable for those living or working in the room, as well as to ensure that energy efficiency was maximized. The student team then proceeded to the lighting room to check the start and stop status of the lighting in each room. This was to determine if there were any lighting fixtures that had been left on for long periods of time, thus wasting energy, or if there were any lighting fixtures that needed to be replaced or repaired. Finally, the student team arrived at the building's top-floor boiler room to check the condition of the hot water supply and heating systems. The aim of this step was to ensure that these systems were providing hot water and heating services properly, but also to assess their energy efficiency in order to seek possible improvements.

Through this building energy audit, the students used professional measurement tools to collect data on the energy consumption of the equipment, which provided strong support for the subsequent analysis. This phase of hands-on practice honed their practical skills and better understand the operation mechanism of the energy system. In the following weeks, the students conducted organization and analysis of the collected data. By applying engineering calculations and systems analysis skills, the students identified potential points of energy waste and opportunities for improvement. This included identifying energy inefficient equipment, suggesting improvements to reduce energy consumption, and performing a quantitative economic benefit

analysis for each improvement project. This analysis phase not only trained them problem-solving skills but also developed the understanding of sustainable energy management.

Finally, the students compiled our findings and recommendations into a formal report. This report not only presented the data and analysis results, but also clearly communicated the value and necessity of each improvement project. Through this process, the students honed their communication and report writing skills, and laid a solid foundation for future professional communication and collaboration in the engineering field. Overall, this program provided them with a valuable hands-on opportunity to apply what they learned in real-world projects, developed problem-solving and teamwork skills, and laid a solid foundation for their future career development in the building energy field.

6.3 High Resolution BEMs Auto-Calibration Tool and Monitoring Software Development

In this project, we developed an advanced automated high-resolution building energy modeling calibration tool based on Python, which brings breakthroughs in research and practice in the field of building energy modeling. This tool not only calibrates building energy models with high accuracy, but also automates the calibration process, greatly improving the efficiency and accuracy of calibration.

We have thoroughly studied the calibration of building energy models and developed a new Bayesian intelligent algorithm to address the shortcomings of the traditional calibration process with tedious parameter adjustment and optimization. The algorithm combines machine learning and Bayesian optimization techniques, and is able to learn the behavioral patterns of the building energy system from a large amount of actual data, and then automatically adjusts the high-resolution BEM parameters so that they are highly compatible with the actual energy consumption trends. This new Bayesian auto-calibration method not only improves the accuracy of calibration, but also dramatically reduces the calibration time, thus saving valuable time and energy for engineers and researchers.

In addition to the auto-calibration tool, we have also developed a building fault monitoring and detection software for the building energy management sector, which is based on advanced data analytics techniques that combine pattern recognition and anomaly detection algorithms. By

monitoring and analyzing real-time data from the building energy system, the software is able to detect anomalies and potential faults in the system in a timely manner, providing early warning and diagnostic information to engineers to help them take prompt action to avoid energy waste and equipment damage. In order to make it easier for engineers to manage and use these tools, we have also developed intuitive and friendly graphical user interfaces (GUIs) for this software. These interfaces not only make the software easier to operate, but also provide intuitive data presentation and analysis functions to help users better understand the operational status and optimization potential of building energy systems.

In summary, through this project, we have not only achieved significant innovations in the field of building energy model calibration and fault detection, but also provided engineers and researchers with a series of powerful tools to help them manage building energy systems more efficiently and achieve sustainable energy use and conservation.

6.4 Journal Paper Publication

In the course of our research, we insisted on a rigorous scientific methodology and adopted an innovative approach to explore the cutting-edge issues in the field under study. Our research team put a great deal of effort into this study, from problem definition and hypothesis construction, to experimental design and data collection, all of which were rigorously planned and implemented.

The results of our research are not only of theoretical importance, but also have potential for practical application. In our article, we describe in detail the methods and techniques we used and their potential value in solving practical problems. We believe that these methods and techniques can provide new ideas and innovative solutions for research and practice in related fields.

As we move to the submission stage, we plan to submit to a leading journal in the building field. Our research is of great importance in the field of building energy, so we are confident that we will be able to successfully publish the article through the rigorous review process. Our research represents an in-depth exploration and innovative thinking of our team in the field we are studying. We firmly believe that our research can bring useful inspiration and impetus to both the academic community and practical applications. We are looking forward to the evaluation and feedback from

our peers, and hope that we can work together with the researchers to promote the progress and development of the field.

7.0 CONCLUSIONS

7.1 Summary

This study presents a novel framework that conducts building and HVAC monitoring by calibrated high-fidelity building energy model. This research fitted a deep learning-based surrogate model to replace physical model in the calibration process. A novel Bayesian calibration framework has been established to reduce the computational burden.

The calibration result show that our developed framework can calibrate heating, cooling, and electricity with the coefficient of variation of the root mean squared error (CVRMSE) are 23.9%, 28.4%,26.9% and the normalized mean biased error (NMBE) are 4.5%,-2.9%,5.5%, satisfy the hourly calibration requirements in the ASHRAE guideline 14.

The fault detection and diagnosis results indicate that the calibrated physics-based model successfully detects seven common building operation faults. A supply air leakage of 30% can lead to an additional 8.6% increase in cooling energy consumption. Similarly, a thermostat measurement bias of 2.2 ℃ can result in an additional 16.9% increase in cooling energy consumption. When dampers are stuck at 30%, there can be an additional 4.9% increase in cooling energy consumption. Additionally, a supply air temperature sensor bias of 2.2 ℃ can result in an additional 15.0% increase in cooling energy consumption. If the air handling unit fan motor experiences a degradation of 30%, it can lead to an additional 7.2% increase in cooling energy consumption. Duct fouling at 30% can result in an additional 4% increase in cooling energy consumption. Lastly, excessive infiltration at 30% can lead to an additional 7.7% increase in cooling energy consumption.

The assessment conducted by the audit team led to three energy-saving recommendations: turn off boilers in the summer, turn off chilled water to AHU in winter, and optimize boiler temperature controls. Additionally, the energy-saving potential of each recommendation was thoroughly evaluated. The analysis outcomes revealed a projected annual utility cost reduction of $16,162, equating to 8.9% of the total annual utility expenses.

For student engagement, one undergraduate student and three PhD students were actively involved in this research, demonstrating their contributions in several ways. Firstly, they gave poster presentations at the seminar to showcase their research findings to their peers. Second, they were actively involved in the energy audits at the site, providing important support for data collection and analysis. In addition, they worked on the development of modeling software, adding innovation and depth to the technical component of the project. Finally, they actively presented their research results in the form of papers to introduce their findings and contributions to the academic community.

7.2 Future Work

Undoubtedly, further enhancements can be made to refine the hourly calibration methods, incorporating physics-based surrogate models, and integrating the calibrated model with various application scenarios. Furthermore, we should also consider designing new evaluation indices and exploring this framework in various building types, scenarios, and indices to enhance its applicability and generalizability.

REFERENCES

[1] Pérez-Lombard L, Ortiz J, Pout C. A review on buildings energy consumption information. Energy Build 2008;40:394–8. https://doi.org/10.1016/j.enbuild.2007.03.007.

[2] Chong A, Gu Y, Jia H. Calibrating building energy simulation models: A review of the basics to guide future work. Energy Build 2021;253:111533. https://doi.org/10.1016/j.enbuild.2021.111533.

[3] Kim Y-S, Heidarinejad M, Dahlhausen M, Srebric J. Building energy model calibration with schedules derived from electricity use data. Appl Energy 2017;190:997–1007. https://doi.org/10.1016/j.apenergy.2016.12.167.

[4] ASHRAE 90.1-2022 (I-P) | ASHRAE Store n.d. https://www.techstreet.com/ashrae/standards/ashrae-90-1-2022-i-p?product_id=2522082 (accessed July 12, 2023).

[5] White Box Technologies Weather Data n.d. http://weather.whiteboxtechnologies.com/ (accessed July 12, 2023).

[6] Fundamentals of Recurrent Neural Network (RNN) and Long Short-Term Memory (LSTM) network - ScienceDirect n.d. https://www.sciencedirect.com/science/article/pii/S0167278919305974 (accessed July 12, 2023).

[7] MATLAB Deep Learning: With Machine Learning, Neural Networks and Artificial Intelligence | SpringerLink n.d. https://link.springer.com/book/10.1007/978-1-4842-2845-6 (accessed July 12, 2023).

[8] Zhang J, Zhao X. A novel dynamic wind farm wake model based on deep learning. Appl Energy 2020;277:115552. https://doi.org/10.1016/j.apenergy.2020.115552.

[9] Im S, Lee J, Cho M. Surrogate modeling of elasto-plastic problems via long short-term memory neural networks and proper orthogonal decomposition. Comput Methods Appl Mech Eng 2021;385:114030. https://doi.org/10.1016/j.cma.2021.114030.

[10] Sainath TN, Vinyals O, Senior A, Sak H. Convolutional, Long Short-Term Memory, fully connected Deep Neural Networks. 2015 IEEE Int. Conf. Acoust. Speech Signal Process. ICASSP, South Brisbane, Queensland, Australia: IEEE; 2015, p. 4580–4. https://doi.org/10.1109/ICASSP.2015.7178838.

[11] Zhang Z, Lv Z, Gan C, Zhu Q. Human action recognition using convolutional LSTM and fully-connected LSTM with different attentions. Neurocomputing 2020;410:304–16. https://doi.org/10.1016/j.neucom.2020.06.032.

[12] Helton JC, Davis FJ. Latin hypercube sampling and the propagation of uncertainty in analyses of complex systems. Reliab Eng Syst Saf 2003;81:23–69. https://doi.org/10.1016/S0951-8320(03)00058-9.

[13] Kennedy MC, O'Hagan A. Bayesian calibration of computer models. J R Stat Soc Ser B Stat Methodol 2001;63:425–64. https://doi.org/10.1111/1467-9868.00294.

[14] Metropolis N, Rosenbluth AW, Rosenbluth MN, Teller AH, Teller E. Equation of State Calculations by Fast Computing Machines. J Chem Phys 1953;21:1087–92. https://doi.org/10.1063/1.1699114.